Dynamical screening effects on Auger *CVV* line shapes of solids

Michele Cini and A. D'Andrea
Istituto Metodologie Avanzate Inorganiche del Consiglio Nazionale delle Ricerche, Casella Postale 20, I-00016 Monterotondo Scalo (Roma), Italy
(Received 25 October 1983)

The current theory of Auger *CVV* spectra of solids takes solid-state polarization effects into account by a statically screened hole-hole repulsion parameter U. Here we include dynamical screening effects by considering a plasmon field coupled to final-state holes interacting through the bare repulsion U_0. We sum the series of diagrams that dominate the two-hole Green's function when the plasma frequency ω_p is large compared with the hopping parameter V between nearest neighbors. Moreover, we show that in this case the theory reduces to a Cini model or a Sawatzky model plus the interaction with a single effective plasmon. This is solved exactly and provides an understanding of various features of the system. Split-off two-hole resonances occur at higher kinetic energies than predicted by the statically screened theory, and under certain resonance conditions they are broadened due to the presence of a preferential decay channel. Bandlike spectra are also significantly modified and the transition between bandlike and atomiclike behavior is characterized by the occurrence of broadened resonances within the band continuum.

I. INTRODUCTION

The current theory of Auger *CVV* spectra of solids successfully explains the occurrence of atomiclike and bandlike features and also gives a fairly good description of the lineshapes of several d-band metals. Essentially the theory reduces to the calculation of the density of states $N_s(\omega)$ of the final-state holes in a tight-binding solid with the inclusion of hole-hole interaction effects. The simplest formulation of the theory[1,2] applies to a completely occupied s valence band. Assuming that the Auger transition occurs at site 0 in the solid, the Cini model includes the hole-hole repulsion by adding to the tight-binding Hamiltonian an interaction term of the form

$$H_I = U n_{0+} n_{0-} , \tag{1}$$

where $n_{i\sigma}$ is the occupation number operator for a hole at site i with spin σ. The model is then solved exactly for the two-hole Green's function. Sawatzky[3] has shown that the model is also solved exactly if an identical repulsion between the holes is allowed for on all sites, and the interaction Hamiltonian is taken to be

$$H_I = U \sum_i n_{i+} n_{i-} . \tag{2}$$

The form (1) appears to be more suitable for an adsorbate or an impurity atom, while the alternative (2) should better describe a perfectly periodic solid. However, Sawatzky and Leselink[4] have found that even in the latter case the results of the two theories are close to each other, apart from a small dispersion broadening of quasiatomic peaks that is absent in the Cini theory.

The extension of the above models to degenerate orbitals[2] and bands[5] is still solved exactly, but the results are obviously much more complicated. However, in many cases the one-particle density matrix $\rho_{ll'}$ is approximately diagonal in angular momentum space and each multiplet component can be treated as an independent s band with a different repulsion parameter U. Using this simplified form of the Cini theory, Weightman and Andrews[6,7] analyzed their high-resolution spectra of a series of transition metals and alloys. In this way they obtained a good representation of the line shapes and extracted empirical values of the repulsion parameters U.

Even if the theory works rather well, it has the obvious shortcoming that the U parameters can only be obtained by comparing theory and experiment, as Madden *et al.*[8] did in the case of Cu. Since they represent repulsion energies in the solid it is clear that they differ from the "bare" repulsion U_0 measured in gas-phase atomic Auger spectra by a relaxation contribution due to solid-state screening. In the case of core spectra the Auger electron kinetic energy is expressed through one- and two-hole extra-atomic relaxation energies that can be obtained[9] by static screening calculations. However, it is not obvious that a static screening calculation is adequate to describe relaxation around a quasiatomic two-hole resonance which is centered around an atom but is not structureless. On the other hand, delocalized bandlike states should test the dielectric response of the solid at frequencies of the order of the bandwidth W, not just the static response. Moreover, the density of states is expected to show intrinsic plasmon satellites that are not borne out by the current theories.

A more general theory including the dynamics of extra-atomic screening explicitly should give a significantly improved line shape expressed directly in terms of the bare repulsion U_0. It is natural to approach this difficult problem by using the Cini or the Sawatzky theory with a bare interaction U_0 as the unperturbed model and adding further terms to the Hamiltonian to represent the coupling of the holes to the elementary excitations of the solid. These are conveniently represented as a field of bosons (plasmons, phonons, or bosonized electron-hole pairs), and here we wish to consider the case when

plasmons dominate the dielectric response. Since the dynamics of the interacting holes are essentially more complicated in the case of open bands,[10] we confine this preliminary investigation to the case when the valence band is completely occupied in the ground state. Thus the present theory is directly relevant to the spectra of insulators, semiconductors, and transition metals with filled d bands, when the plasmons are mainly due to the conduction sp band.

In Sec. II we propose an extended model that is basically a Cini or Sawatzky model with the addition of a plasmon field. We perform a diagrammatic analysis of the perturbation expansion. Commonly, the plasmon energy ω_p is much larger than the tight-binding hopping parameter V, and we select the class of diagrams that dominates the perturbation series in this case. Hence we show that we can replace the plasmon field by a single effective boson mode. In Sec. III we solve the one-boson model exactly. Then we are in a position to discuss the effects of dynamical screening and we do so in Sec. IV, where we illustrate a rich phenomenology by selected examples. The physical conclusions are summarized in Sec. V.

II. FORMULATION

A. Extended Cini and Sawatzky models

Let the Hamiltonian for the two bare interacting valence holes be

$$H_b = H_{\rm tb} + H_I \ , \tag{3}$$

where $H_{\rm tb}$ is a tight-binding model for a solid with an s band and nearest-neighbor hopping parameter V, and H_I is a hole-hole repulsion term appropriate to the Cini or the Sawatzky model but with the bare, gas-phase repulsion parameter U_0 in place of the statically screened U. The plasmon field and its interaction with the holes is then described within the tight-binding approach by

$$H' = H_p + H_{h\text{-}p} \ , \tag{4}$$

where the free-plasmon term is

$$H_p = \sum_q \omega_q b_q^\dagger b_q \ , \tag{5}$$

and the coupling term is linear in the plasmon operators,

$$H_{h\text{-}p} = \sum_q g_q \sum_{i,\sigma} \exp(i\vec{q}\cdot\vec{R}_i) n_{i\sigma} b_q^\dagger + \text{H.c.} \tag{6}$$

Here $n_{i\sigma}$ is the occupation-number operator for a valence hole at site i with spin σ, and $g_q \exp(i\vec{q}\cdot\vec{R}_i)$ is its coupling with a plasmon of wave vector $\vec{q}$, frequency ω_q, and creation operator $b_q^\dagger$. We may take[11,12] $g_q^2 = (2\pi\omega_q/q^2\Omega)$, where Ω is a normalization volume independent[13] of the atomic (core or valence) state of the hole. The $\vec{q}$ summations have an upper cutoff q_c of the order of the inverse of the static screening length. In the models of Cini and Sawatzky and also in the bare Hamiltonian (3) the two valence holes interact only when they belong to the same atom. To be physically consistent we must assume a large q_c, which implies that in the core limit of the theory ($V \to 0$) the static screening is short ranged. To express this mathematically we consider two core holes at sites i and j. The relaxation shift is

$$\Delta E(i,j) = \sum_q g_q^2 \, |\exp(i\vec{q}\cdot\vec{R}_i) + \exp(i\vec{q}\cdot\vec{R}_j)|^2/\omega_q \tag{7}$$

and when q_c is large this becomes simply

$$\Delta E(i,j) = \sum_q g_q^2 (2 + 2\delta_{ij})/\omega_q \ . \tag{8}$$

In other words, the two holes are screened as a double charge if they belong to the same atom, otherwise they are screened independently.

If the primary ionization produces a core hole at site 0 with occupation number operator n_c, this is coupled to the plasmon field by a further term of the form

$$H_c = \sum_q g_q (b_q^\dagger + b_q) n_c \ . \tag{9}$$

Dynamical interference effects between the primary hole and the Auger holes can only be described in a "one-step"[14,15] formulation of the theory. For the case of valence holes this work is currently under way; here we restrict our attention to the case when the core-hole lifetime is long and the Auger spectrum can be studied in the two-step model. Therefore, we consider the evolution of the system with the "extended Hamiltonian" $H_{\rm EM} = H_b + H'$, while the effect of H_c is to prepare a fully relaxed, coherent plasmon state $|c\rangle$ as the initial state for the Auger transition. The coherent state $|c\rangle$ is obtained from the vacuum $|v\rangle$ by applying the operator[16]

$$X = \exp\left[\sum_q g_q (b_q - b_q^\dagger)/\omega_q\right] . \tag{10}$$

We denote by $|i,j\rangle$ the configuration with the up-spin hole at site i and the down-spin hole at site j in the absence of the boson degrees of freedom and $|ijv\rangle$ the same hole configuration with the plasmon vacuum. The two-hole density of states $N_d(\omega)$ including dynamical screening effects is $(-\pi)^{-1}$ times the imaginary part of the Green's function

$$G(0,0;0,0;\omega) = \langle 0,0,v \,|\, X^\dagger (\omega - H_{\rm EM})^{-1} X \,|\, 0,0,v\rangle \ , \tag{11}$$

where ω has a vanishingly small positive imaginary part.

It is apparent on physical grounds, and we shall prove below that in the limit $\omega_q \to \infty$, when the solid-state screening may be regarded as instantaneous, this formulation should return a statically screened model of the Cini or Sawatzky form. When we want to include the plasmon dynamics explicitly the problem looks very complicated, since there is a huge number of plasmon variables. Even if at the present stage there is ample justification in neglecting plasmon dispersion in energy ($\omega_q \equiv \omega_p$) we must necessarily deal with the spatial dispersion. This means that for each $\vec{q}$ value there is an independent harmonic oscillator that can be in any of its allowed states, and it is difficult to keep track of all these degrees of freedom. Physical reasoning is useful to proceed and an important indication comes from the core limit of the theory, when the $n_{i\sigma}$ are good quantum numbers. Then the density of states associated with the sudden switching of an arbitrary charge distribution can also be obtained by

replacing the plasmon field with a single plasmon mode with an effective coupling constant g, as is obvious from Langreth's treatment.[16] We stress here that the single mode gives quite a poor description of the dynamics of the plasmon field, yet it allows the description of the dynamics of the core holes correctly, and the resulting density of states is exact.

Here we cannot content ourselves with the core limit because the valence degrees of freedom are essential to us, however, we want to know whether a similar simplification arises in the valence case when $\lambda = V/\omega_p$ is small. This is the case of practical interest since most often the plasmon energy is larger than the bandwidth W, and W is many times the hopping parameter V in the three-dimensional lattices.[17] Therefore we set up the diagrammatic analysis of the perturbation series for G in powers of the g_9 coupling, then select the class of diagrams that are dominant for $\lambda \ll 1$ and sum them to infinite order.

Using the operator identity

$$\exp(A+B)=\exp(A)\exp(B)\exp(-1/2[A,B]) ,$$

valid when $[A,B]$ is a c number, we develop the X operator and obtain

$$G(0,0;0,0;\omega)=\exp(-a)\langle 0,0,v \mid \exp\left[-\sum_q g_q b_q/\omega_p\right] \times(\omega-H)^{-1}\exp\left[-\sum_q g_q b_q^\dagger/\omega_p\right] \mid 0,0,v\rangle , \tag{12}$$

with $a=\sum_q g_q^2/\omega_p^2$.

Then expanding the resolvent operator we cast the formal series for G in the form

$$G=\exp(-a)\sum_k \sum_{m,n} \psi_{mn}^{(k)}/m!n! , \tag{13}$$

where

$$\psi_{mn}^{(k)}=\langle 0,0,v \mid \left[-\sum_q g_q b_q/\omega_p\right]^m \frac{1}{\omega-H_b-H_p} \times \left[H_{h\text{-}p}\frac{1}{\omega-H_b-H_p}\right]^k \left[-\sum_q g_q b_q^\dagger/\omega_p\right]^n \mid 0,0,v\rangle . \tag{14}$$

Since the problem involves two holes of opposite spin in a closed band, the diagrammatic analysis is made easier if we have $H_{h\text{-}p}$ in the equivalent two-body form:

$$H_{h\text{-}p}=\sum_q g_q \sum_{i,j}[\exp(i\vec{q}\cdot\vec{R}_i)+\exp(i\vec{q}\cdot\vec{R}_j)]n_{i+}n_{j-}b_q^\dagger+\text{H.c.} \tag{15}$$

and note that $n_{i+}n_{j-}$ is a projection operator that selects one hole configuration. The diagrams are drawn as follows. The propagation of two holes interacting with the bare repulsion U_0 can be represented as a single straight line spanning the space of two-hole configurations. We then draw a straight line connecting two circles, choose k points along it, and label each of them by a two-hole configuration ij. The two end points belong to the configuration 00. Then, we draw plasmon lines joining two configurations, or a configuration and one of the circles. Lines joining the two circles directly are also admitted. Every intermediate configuration has one plasmon line entering or leaving it, but m lines come out of the left-hand circle and n lines end at the right circle.

Since at every interaction the sum of the frequencies of the two-hole line and the boson lines is conserved, to every segment of the straight line there corresponds a factor $G^0(i,j;\,k,l;\,\omega-s\omega_p)$, where G^0 is the bare Green's function, ij and kl are the left and right configurations, and s is the number of plasmon lines present in the prescribed interval. Every plasmon line joining the two circles directly brings a factor $a=\sum_q g_q^2/\omega_p^2$. Every plasmon line connecting two configurations i,j and k,l brings a factor

$$F(i,j;k,l)=\sum_q g_q^2[\exp(-i\vec{q}\cdot\vec{R}_i)+\exp(-i\vec{q}\cdot\vec{R}_j)] \times[\exp(i\vec{q}\cdot\vec{R}_k)+\exp(i\vec{q}\cdot\vec{R}_l)] . \tag{16}$$

A plasmon line connecting the point labeled i,j with the left-hand circle brings a factor

$$f(i,j)=\sum_q g_q^2[\exp(i\vec{q}\cdot\vec{R}_i)+\exp(i\vec{q}\cdot\vec{R}_j)]/\omega_p . \tag{17}$$

Equation (17) becomes $f^*(i,j)$ if the plasmon line reaches the right-hand circle instead. Every diagram is multiplied by $(-1)^{m-n}$. Finally, each diagram carries a combinatorial factor $m!n!/r!$, where r is the number of plasmon lines joining the two circles directly.

For example, Fig. 1(a) contributes to $\psi_{22}^{(0)}$ and yields

$$2G^0(0,0;0,0;\omega-2\omega_p)a^2 , \tag{18}$$

Fig. 1(b) contributes to $\psi_{12}^{(1)}$ and yields

$$-2G^0(0,0;i,j;\omega-\omega_p)G^0(i,j;0,0;\omega-2\omega_p)af^*(i,j) , \tag{19}$$

and Fig. 1(c) contributes to $\psi_{11}^{(2)}$ by

$$aG^0(0,0;i,j;\omega-\omega_p)G^0(i,j;k,l;\omega-2\omega_p) \times G^0(k,l;0,0;\omega-\omega_p)F(i,j;k,l) . \tag{20}$$

After summing over intermediate two-hole configurations, the sum of all diagrams with k internal points gives $\psi_{mn}^{(k)}$. Then, G is obtained from Eq. (13). From the complete perturbation series we now select the diagrams of

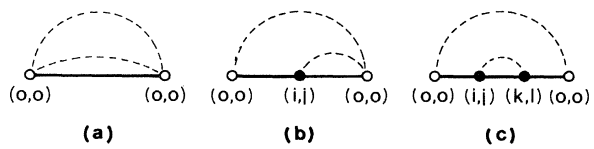

FIG. 1. Typical diagrams for the Green's function of two interacting holes screened by a plasmon field. The straight line represents the bare Green's function G^0; the dots along it stand for two-hole configurations where plasmons (dotted lines) are emitted or absorbed. The two end circles allow for plasmon excitations due to the primary core hole. The explicit contributions of (a), (b), and (c) are given in Eqs. (18), (19), and (20), respectively.

lowest order in $\lambda=V/\omega_p$. We are interested in $G(\omega)$ when ω is in the band region. Then we note that G^0 is essentially configuration diagonal when calculated at large frequencies of order $\omega_p \gg V$ (or several times ω_p), or, in other words,

$$G^0(i,j;m,n;\omega-s\omega_p)\simeq\delta_{im}\delta_{jn}G^0(i,j;i,j;\omega-s\omega_p) \quad s>0 . \tag{21}$$

Off-diagonal terms are smaller than the diagonal ones by a factor of order $(\lambda/s)^p$, where p is the minimum number of hops needed to reach the i,j hole configuration starting from the m,n configuration. Therefore, the dominant diagrams for $\lambda \ll 1$ are those where the bare Green's functions of argument $\omega-s\omega_p$ with $s>0$ are diagonal in hole configuration, while off-diagonal Green's functions of argument ω are of course allowed. Physically, this reflects our assumption that plasmons are much faster variables than the holes. A virtual plasmon can exist for times of the order ω_p^{-1}, and it is unlikely that the hole configuration changes on this time scale.

Therefore if $\lambda \ll 1$, G reduces to the sum (to all orders) of the dominant class of diagrams obtained by inserting the restriction (21) into the full perturbation series. Here we shall show how this summation is performed. However, the main use of the above analysis is to achieve a substantial physical simplification of the theory that is justified for $\lambda \ll 1$. We wish to show that we can indeed replace the plasmon field by a single effective boson, in analogy with the core case. The resulting one-boson model is a close approximation to the extended model for small λ because the dominant diagrams of the two models are the same, and we can solve it exactly. Therefore it shares the distinct advantages of exactly solved theories including a more direct interpretation of the physical assumptions than approximate treatments allow and a wider applicability to different contents. As a by-product of its solution we shall also find the sum of the partial series for the extended model.

At this point we may take the hole-hole bare interaction to be local in real space (Cini theory) or in the lattice Fourier-transform $\vec{K}$ space (Sawatzky theory). The two alternatives can be developed in parallel and to avoid duplication of most of the formalism we adopt the latter choice in the following section. The limit when the two-hole dispersion vanishes will be given in Sec. IV.

B. Fast-plasmon limit and the one-boson model

Let the model Hamiltonian be $H_{\rm OB}=H_b+H_p+H_{h\text{-}p}$, where H_b is a Hubbard model with the bare interaction U_0, while the boson-dependent terms are replaced by

$$H_p=\omega_p b^\dagger b , \tag{22}$$

$$H_{h\text{-}p}=\left[2g_0\sum_i n_{i+}n_{i-}+g_0\sqrt{2}\left[1-\sum_i n_{i+}n_{i-}\right]\right]\times(b+b^\dagger) . \tag{23}$$

The coherent initial state due to the primary core hole is obtained from the plasmon vacuum by applying the operator $X(1)$, where

$$X(\mu)=\exp[\mu g_0(b-b^\dagger)/\omega_p] , \tag{24}$$

and the dressed two-hole Green's function is of the form (11) with $X(1)$ in place of X and $H_{\rm OB}$ in place of $H_{\rm EM}$. The diagrams for the Green's function are the same as for the extended model and the class of leading diagrams for $\lambda=V/\omega_p \ll 1$ also remains unaltered. Moreover, each leading diagram has exactly the same value in the two theories if the effective coupling g is chosen such that $g_0^2/\omega_p^2=a$. Indeed in the leading diagrams only the configuration diagonal factors $F(ij,ij)$ and $f(0,0)$ appear, and in view of Eqs. (7) and (8), these are the same for the two models.

Therefore the one-boson model coincides with the extended model to leading order in λ and contains the most important coherence effects on the motion of the two holes (in real and in frequency space) that are induced by plasmon dispersion. The main effect is that the holes are screened independently if they are on different atoms but as a double charge if they are on the same site. However, what we have obtained is much more than the core limit of the theory, and the final results still depend on the full G matrix.

Here we wish to compare the results of the dynamical theory with those of the "statically screened" theory that corresponds to the limit $\lambda=0$. The "static" theory assumes instantaneous screening and can be obtained by applying the Born-Oppenheimer principle in reverse,[18] the fast variables being boson rather than electron coordinates. The two-hole motion in the average potential due to the plasmons is described by an effective bosonless Hamiltonian $H_{\rm eff}$ and the mean plasmon potential is obtained by averaging the boson operators over the completely relaxed, coherent state that corresponds to the instantaneous holes configuration. If we let

$$P=\sum_i n_{i+}n_{i-}, \quad Q=1-P , \tag{25}$$

we may write $H_{\rm OB}$ in the form

$$H_{\rm OB}=H_{\rm tb}+P[U_0+\omega_p b^\dagger b+2g_0(b^\dagger+b)]+Q[\omega_p b^\dagger b+g_0\sqrt{2}(b^\dagger+b)] . \tag{26}$$

The effective Hamiltonian for the holes is then

$$H_{\rm eff}=H_{\rm tb}+P(U_0+\omega_p\langle b^\dagger b\rangle_p+2g_0\langle b^\dagger+b\rangle_p)+Q(\omega_p\langle b^\dagger b\rangle_Q+g_0\sqrt{2}\langle b^\dagger+b\rangle_Q) , \tag{27}$$

where $\langle\ \rangle_p$ denotes the expectation value over the vacuum of the operator b_0+2g_0/ω_p, and the same for $\langle\ \rangle_Q$ of the operator $b_0+g_0\sqrt{2}/\omega_p$. Hence,

$$H_{\rm eff}=H_{\rm tb}+U_sP-\delta , \tag{28}$$

where $\delta=2g_0^2/\omega_p$ is a general shift of all the eigenvalues, and the statically screened repulsion

$$U_s=U_0-2g_0^2/\omega_p \tag{29}$$

can be identified with the U parameter of the current theories.

Before proceeding with the solution we wish to point

out that a nontrivial distortion of the line shapes due to plasmon dynamics was predicted by one of us[19] in a theory of core-core-valence Auger spectra. Up to now those results have not been tested against experiment, essentially because intensity problems make it difficult to obtain experimental line shapes of adequate quality. The case of core-valence-valence spectra that we are considering here should definitely be much more favorable in this respect. On the other hand, the theory is obviously more complex and requires a substantial development of the mathematical technique introduced in Ref. 19, as will be apparent in the next section.

III. SOLUTION

To evaluate the two-hole local Green's function

$$G(0,0;0,0;\omega)=\langle 0,0,v \mid X^{\dagger}(1)(\omega-H_{\mathrm{OB}})^{-1}X(1) \mid 0,0,v\rangle \ , \tag{30}$$

we find it convenient to introduce the canonically transformed Hamiltonian

$$\tilde{H}=X^{\dagger}(\sqrt{2})H_{\mathrm{OB}}X(\sqrt{2})=\tilde{H}_b+H_p+\tilde{H}_{h\text{-}p} \ . \tag{31}$$

According to the definition of Eq. (24) one finds

$$\tilde{H}_b=H_{\mathrm{tb}}+U_d\sum_i n_{i+}n_{i-}-\delta \ , \tag{32}$$

where U_d is given by

$$U_d=U_0-4(\sqrt{2}-1)g_0^2/\omega_p \tag{33}$$

and differs from the statically screened repulsion U_s of Eq. (29), while the shift is the same as in Eq. (28), namely,

$$\delta=-2g_0^2/\omega_p \ . \tag{34}$$

The transformed hole-plasmon interaction term reads

$$\tilde{H}_{h\text{-}p}=g\sum_i n_{i+}n_{i-}(b+b^{\dagger}) \ , \tag{35}$$

with

$$g=(2-\sqrt{2})g_0 \ . \tag{36}$$

Also, let

$$\gamma=g_0(\sqrt{2}-1) \ . \tag{37}$$

Since obviously $X^{\dagger}(\sqrt{2})X(1)=X^{\dagger}(\sqrt{2}-1)$, we may cast the Green's function in the form

$$G(0,0;0,0;\omega)=\langle\tilde{\tau}\mid(\omega-\tilde{H})^{-1}\mid\tilde{\tau}\rangle \tag{38}$$

with

$$\begin{aligned}\mid\tilde{\tau}\rangle&=X^{\dagger}(\sqrt{2}-1)\mid 0,0,v\rangle\\&=\exp(-\gamma^2/2\omega_p^2)\sum_{n=0}^{\infty}\left[\frac{\gamma}{\omega_p}\right]^n\frac{(b^{\dagger})^n}{n!}\mid 0,0,v\rangle \ .\end{aligned} \tag{39}$$

Therefore we may write

$$G(0,0;0,0;\omega)=\exp(-\gamma^2/\omega_p^2)\times\sum_{m=0}^{\infty}\sum_{n=0}^{\infty}\left[\frac{\gamma}{\omega_p}\right]^{m+n}\frac{1}{m!n!}\phi_{mn}(0,\omega) \ , \tag{40}$$

where we have introduced the quantities

$$\phi_{mn}(i,\omega)=\langle i,i,v\mid b^m(\omega-\tilde{H})^{-1}(b^{\dagger})^n\mid 0,0,v\rangle \ . \tag{41}$$

Consider the expectation value over $\mid 0,0,v\rangle$ of the operator identity

$$b^m(\omega-\tilde{H})^{-1}(b^{\dagger})^n=b^m(\omega-H_0)^{-1}(b^{\dagger})^n+b^m(\omega-H_0)^{-1}H_1(\omega-\tilde{H})^{-1}(b^{\dagger})^n \tag{42}$$

with $H_0=\tilde{H}_b+H_p$ and $H_1=\tilde{H}_{h\text{-}p}$. Using

$$b^mH_0=(H_0+m\omega_p)b^m \tag{43}$$

and the commutation rule for the boson operators we readily derive the recurrence relations

$$\phi_{mn}(0,\omega)=m!\delta_{mn}D^0(0,0;0,0;\omega-m\omega_p)+g\sum_i D^0(0,0;i,i;\omega-m\omega_p)\times[\phi_{m+1\,n}(i,\omega)+m\phi_{m-1\,n}(i,\omega)] \ , \tag{44}$$

where D^0 is the Green's function for $g=0$. Note that D^0 is computed from $\tilde{H}_b$ and should not be confused with the bare Green's function G^0. In terms of the lattice Fourier transforms

$$\phi_{mn}(K,\omega)=\sum_i\phi_{mn}(i,\omega)\exp(-i\vec{K}\cdot\vec{R}_i) \ , \tag{45}$$

$$D^0(K,\omega)=\sum_i D^0(0,0;i,i;\omega)\exp(i\vec{K}\cdot\vec{R}_i) \ , \tag{46}$$

and with the shorthand notation

$$D_m^K=D^0(K;\omega-m\omega_p) \ , \tag{47}$$

the recurrence relations become

$$\phi_{mn}(K,\omega)=D_m^K\{m!\delta_{mn}+g[\phi_{m+1\,n}(K,\omega)+m\phi_{m-1\,n}(K,\omega)]\} \ . \tag{48}$$

For $m>0$ let us introduce the finite continued fractions

$$A_m^K=gD_{m-1}^K/[1-(m-1)g^2D_{m-1}^KD_{m-2}^K/(1-\cdots)] \tag{49}$$

that terminate after $m-1$ denominators. Also we need the infinite continued fractions

$$B_m^K=(m+1)gD_{m+1}^K/[1-(m+2)g^2D_{m+1}^K\times D_{m+2}^K/(1-\cdots)] \ . \tag{50}$$

Solving Eqs. (48) one finds that

$$\phi_{mn}(K,\omega)=A_{m+1}^KA_{m+2}^K\cdots A_n^K\phi_{nn}(K,\omega), \quad m<n \tag{51}$$

and

$$\phi_{mn}(K,\omega)=B^K_{m-1}B^K_{m-2}\cdots B^K_n\phi_{nn}(K,\omega),\quad m>n \tag{52}$$

while the diagonal elements are given by

$$\phi_{nn}(K,\omega)=\frac{n!D^K_n}{1-gD^K_n(B^K_n+nA^K_n)}\ . \tag{53}$$

Thus the ϕ matrix is expressed in terms of $D^0(K,\omega)$ and in view of Eq. (40) this is what we need to solve the one-boson model. If instead we wish to solve the extended model for $\lambda\ll 1$ the above results should first be expressed in terms of the bare Green's function G^0, which is achieved through the relation

$$D(K,\omega)=\frac{G^0(K,\omega+\delta)}{1-\Delta U\,G^0(K,\omega+\delta)}\ , \tag{54}$$

where $\Delta U=U_d-U_0$ and $G^0(K,\omega)$ is the lattice Fourier transform of G^0 analogous to Eq. (46). The class of dominant diagrams for $\lambda\ll 1$ is selected by the restriction (21), which leads to the following when inserted into Eq. (54):

$$D^K_m=D^0(0,0;0,0;\omega-m\omega_p),\quad m>0\ , \tag{55}$$

where the right-hand side is K independent.

Since, as shown in Sec. II, both theories have the same dominant diagrams and values, if we adopt the ansatz (55) in the solution of the one-boson model, we solve the extended model for $\lambda\ll 1$. In the rest of this paper we shall deal exclusively with the exact solution of the one-boson model. In any case, the solution for both models is completed by an inverse Fourier transformation

$$\phi_{mn}(0,\omega)=\frac{1}{N}\sum_K\phi_{mn}(K,\omega)\ . \tag{56}$$

IV. DISCUSSION

The Auger line shapes predicted by the dynamically screened theory differ significantly and sometimes even qualitatively from those of the "static" theory and we wish to illustrate the main effects here by selected numerical examples. In practice, we can avoid the laborious K summation of Eq. (56). As in the static Cini model, we may neglect the dispersion of the two-hole bound state, which amounts to dropping the K indices in Eqs. (47)—(53) and referring all quantities to site 0, where the Auger decay occurs. As discussed in the Introduction, this is a natural approach to impurity problems where no translational symmetry exists and is a very convenient approximation when applied to crystals. With this simplification, the algorithm of Sec. III proved to be fast and efficient and we never met convergence troubles with the continued fractions nor with the double infinite summations of Eq. (40).

The dynamical effects we are interested in are understood more readily if the noninteracting one-particle density of states $\rho(\omega)$ is taken to be simple and symmetric. As in previous work we exemplify the results with a rectangular level shape

$$\rho(\omega)=\Theta(\alpha-|\omega|)/2\alpha\ , \tag{57}$$

which allows computation of the two-hole Green's function D^0 of Eq. (44) in closed analytical form.[2]

In order to substantiate the dynamical effects we wish to contrast the two-hole density of states $N_d(\omega)$ of the one-boson model with its static screening limit $N_s(\omega)$. We have shown in Sec. III B that the theory does have a well-defined static limit, with a Hamiltonian (28) of the Cini or Sawatzky form where the repulsion parameter should be identified with the statically screened U_s of Eq. (29). Then we know[2] that if $\gamma=U_s/\alpha$ is well above a critical value γ_c a split-off quasiatomic peak dominates $N_s(\omega)$. For the rectangular $\rho(\omega)$, $\gamma_c\simeq 1.44$. This is the quasiatomic situation common in narrow-band materials. For example, by using the "typical" values $\alpha=3.5$ eV and $U_s=7$ eV, then $\gamma=2$ and the splitoff resonance is as shown in Fig. 2 (curve S). The resonance has a finite width because the imaginary part of ω was given a finite value Γ for numerical convenience, the dotted line represents the density of states in the independent particle limit, while the residual bandlike part of the spectrum is weak and is not shown.

Since the quasiatomic peak represents a spatially localized bound state, one could perhaps argue that dynamical screening effects are no more important here than in the case of core spectra. However, this conclusion is correct only in the limit $\omega_p\to\infty$. Consider the case when $U_s=7$ eV arises from the physically reasonable set of parameters $U_0=15$ eV, $\Delta E=g_0^2/\omega_p=4$ eV, and $\omega_p=15$ eV; then the one-boson model yields the split off state labeled D in Fig. 2. The lower intensity of the peak is mostly due to the presence of plasmon satellites outside the energy range of the figure. It is remarkable, however, that the static theory predicts the position of the peak with an error of about 1 eV, and of course the error increases if ω_p is reduced. Yet if ω_p is sufficiently large one can still manage to fit the spectrum within the static theory by using U_s as an adjustable parameter. However, if ω_p is decreased to the point that the resonance condition $\omega_p\simeq U_s$ is met, the

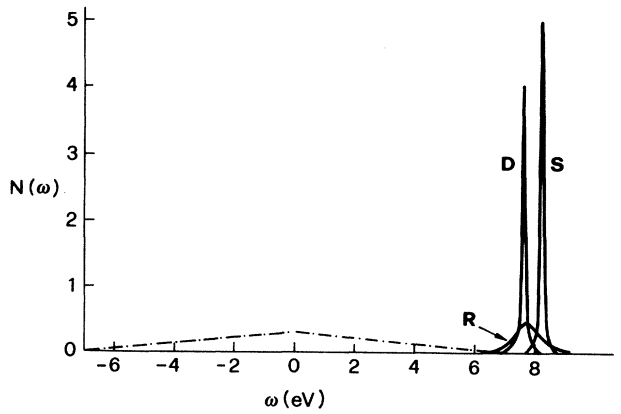

FIG. 2. Comparison of static and dynamical theories in a quasiatomic case. The dotted-dashed line is the self-convolution of the bare, rectangular one-particle density of states, while curve D shows the quasiatomic peak as calculated by the dynamical theory with the input parameters $U_0=15$ eV, $g_0^2/\omega_p=4$ eV, $W=7$ eV, $\Gamma=0.05$ eV, and $\omega_p=15$ eV. Curve R has the same input parameters, except $\omega_p=7.5$ eV. Curve S shows the results of the static theory.

fitting procedure fails completely. For example, if we change the plasmon energy to $\omega_p = 7.5$ eV, while keeping W, U_0, and ΔE fixed, the dynamically screened peak (curve R) broadens dramatically.

This phenomenon is due to the opening of a decay channel for the two-hole bound state that can delocalize into the band continuum by emitting a plasmon. In a recent paper[20] the extended model was solved to second order in g_0 and an estimate was given of the width at half maximum of the quasiatomic peak in the resonant case. Also, we have provided evidence that the resonant mechanism makes an important contribution to the observed width in the case of silver. The approximate treatment of the extended model and exact solution of the one-boson model support each other. For instance, in case of a simple cubic crystal we estimated[20] the full width at half maximum in the resonant case to be

$$\eta \simeq \frac{\pi}{6} \frac{W}{U_0} \frac{g_0^2}{\omega_p} . \tag{58}$$

With the present values of the parameters this is 0.78 eV, in excellent agreement with the exact solution of the one-boson model ($\eta \simeq 0.75$ eV). Thus, dynamical effects are important for a quantitative understanding of quasiatomic spectra, and can also change them qualitatively when $\omega_p \simeq U_s$.[21]

When γ is well below γ_c, say $\gamma = 0.8$, N_s has a broad and deformed bandlike appearence,[2] shown in the curve S of Fig. 3. With $U_0 = 15$ eV, $\Delta E = g_0^2/\omega_p = 4$ eV, $\omega_p = 15$ eV, $\gamma = 0.8$ is reached when $W = 2\alpha = 17.5$ eV. The one-boson model with this set of parameters generates the line shape labeled D in the same figure, which is different in several important details. There is an "intrinsic" plasmon satellite centered at about $\omega = 25$ eV that does not reproduce the shape of the main peak, the positions of the maxima of the D and S curves differ by as much as 1.4 eV, and the D line shape is significantly sharper. While extrinsic processes contribute heavily to the intensity of the experimentally observed satellites, the distortion of the band continuum is an essentially intrinsic effect. By comparing theoretical and experimental line shapes in principle we can obtain an independent estimate of the hole-plasmon coupling g_0.

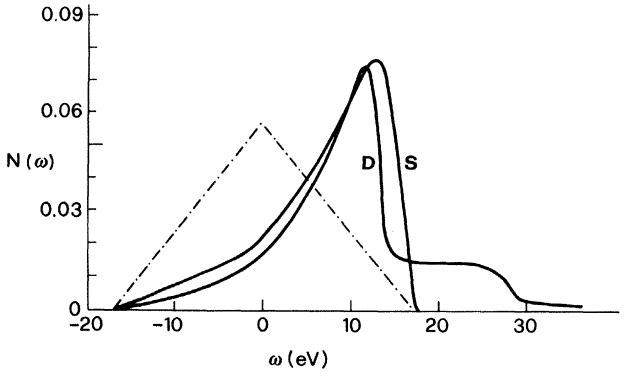

FIG. 3. Two-hole density of states in a bandlike case. The input parameters are $U_0 = 15$ eV, $g_0^2/\omega_p = 4$ eV, $W = 17.5$ eV, $\Gamma = 0.05$ eV, and $\omega_p = 15$ eV. Curves D and S are the line shapes calculated by the dynamical and static theories, respectively.

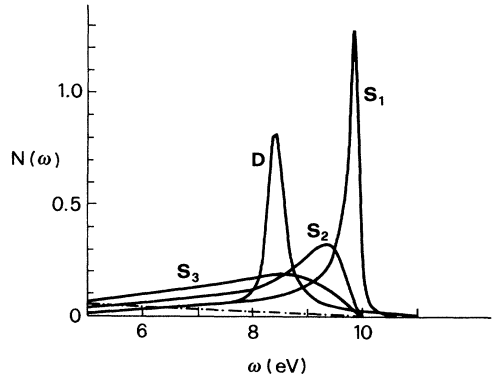

FIG. 4. Two-hole density of states in an intermediate case. Curves D and S_1 show the results of the dynamical and static theories, respectively, with $U_0 = 15$ eV, $g_0^2/\omega_p = 4$ eV, $W = 10$ eV, $\Gamma = 0.05$ eV, and $\omega_p = 15$ eV. If we reduce the U_0 parameter of the static theory [see Eqs. (28) and (29)] to approach the dynamical result we obtain curves S_2 (for $U_0 = 14$ eV) and S_3 (for $U_0 = 13$ eV). When the peak positions agree, the static line shape is essentially bandlike.

The case when $\gamma \simeq \gamma_c$ is also of interest. One such situation is represented in Fig. 4, where $W = 10$ eV, $U_s = 7.0$ eV, and therefore $\gamma = 1.4$. The origin of energies is at the center of the triangular, independent particle line shape, and the spectral region of two-hole resonances is shown. Compare the line shape S_1 resulting from the static theory with the exact result D of the dynamical model. The energy difference between the maxima is very large and the dynamical peak is essentially symmetric. Evidently it represents a true resonance within the continuum, rather than a deformed continuum as in the static theory. The curve D cannot even be approximated by reducing the repulsion parameter in the static theory, because then the line shape tends to become bandlike (curve S_2) and when the maxima are brought in coincidence (curve S_3), the two line shapes are completely different. Thus, if γ is close to γ_c the static theory is inadequate even if U is used as a fit parameter.

V. CONCLUSIONS

Since in most solids the plasmon frequency ω_p is much larger than the hopping frequency between nearest neighbors, we could justify the adoption of a one-boson model to discuss dynamical screening effects on Auger CVV spectra. Imposing the restriction of completely occupied valence bands, we solved the model exactly for the two-hole Green's function. The current theories of Auger line shapes that assume static screening are recovered in the limit $\omega_p \to \infty$.

For the purpose of illustration, we have taken a rectangular one-hole density of states as the noninteracting limit and we have compared the results of static and dynamical theories. The line shapes predicted by the dynamical calculation differ qualitatively from their static counterparts when the spectrum is intermediate between

bandlike and atomiclike. Also, the dynamical theory leads to the prediction of a resonant broadening of quasiatomic splitoff states when $\omega_p \simeq U_s$ and to the interesting possibility that different multiplet components have different widths. Apart from these two cases, the current theory is found to be qualitatively correct, but dynamical effects are generally important. For bandlike and atomiclike spectra as well, the peak positions calculated with the dynamical theory differ significantly and systematically from those of the static theory, where the U_s parameter is expressed in terms of the gas-phase repulsion U_0 and a statical extra-atomic relaxation energy. Even if we use the static theory with U_s as an adjustable parameter we cannot optimize simultaneously the position of the maximum and the width of bandlike features. We stress that the distortion of bandlike line shapes by the plasmons is a purely intrinsic effect, while the analysis of plasmon satellites is complicated by the presence of extrinsic contributions. Therefore, by comparing calculated and experimental spectra we could deduce the strength of the hole-plasmon coupling, a quantity that is not readily accessible by other means. In conclusion, the static theory is a useful first approximation to the overall line shape in most cases, but the dynamical theory is needed if we wish to reach a more advanced, quantitative stage.

[1]M. Cini, Solid State Commun. 20, 605 (1976).
[2]M. Cini, Solid State Commun. 24, 681 (1977).
[3]G. A. Sawatzky, Phys. Rev. Lett. 39, 504 (1977).
[4]G. A. Sawatzky and A. Leselink, Phys. Rev. B 21, 1790 (1980).
[5]M. Cini, Phys. Rev. B 17, 2788 (1978).
[6]P. Weightman and P. T. Andrews, J. Phys. C 13, 3529 (1980).
[7]P. Weightman and P. T. Andrews, J. Phys. C 13, L815 (1980).
[8]H. H. Madden, D. M. Zehner, and J. R. Noonan, Phys. Rev. B 17, 3074 (1978); 18, 2023 (1978).
[9]R. Weissmann and K. Muller, Surf. Sci. Rep. 105, 251 (1981).
[10]M. Cini, Surf. Sci. 87, 483 (1979).
[11]J. I. Gersten, Phys. Rev. 188, 774 (1969).
[12]P. J. Feibelman, C. B. Duke, and A. Bagchi, Phys. Rev. B 5, 2436 (1972).
[13]P. Weightman, J. Phys. C 9, 1117 (1976).
[14]O. Gunnarsson and K. Schönhammer, Phys. Rev. B 22, 3710 (1980).
[15]O. Gunnarsson, K. Schönhammer, J. C. Fuggle, and R. Lässer, Phys. Rev. B 23, 4350 (1981).
[16]D. C. Langreth, Phys. Rev. B 1, 471 (1970).
[17]E. N. Economou, *Green's Functions in Quantum Physics* (Springer, Berlin, 1979), Chap. 5.
[18]D. C. Langreth, Phys. Rev. Lett. 26, 1229 (1971).
[19]M. Cini, Phys. Rev. B 17, 2486 (1978).
[20]M. Cini and A. D'Andrea, J. Phys. C 16, 4469 (1983).
[21]The resonant broadening is comparable to the broadening produced by the core-hole decay, and a more satisfactory estimate of the various contributions to the width probably requires a one-step description of the process.